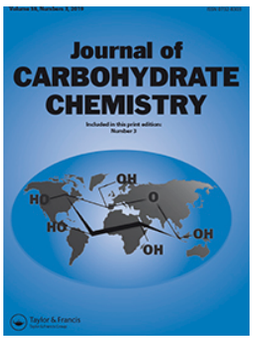

Journal of Carbohydrate Chemistry

ISSN: 0732-8303 (Print) 1532-2327 (Online) Journal homepage: https://www.tandfonline.com/loi/lcar20

Improved synthesis, X-ray structure, and antifungal activity of a sugar-psoralen conjugate: 4,4'-Dimethylxanthotoxol 2,3,4,6-tetra-*O*-Acetyl-β-*D*-glucoside

Chao-Yue Chen, Ting-Hai Yang, Chang-Duo Pan & Xin Wang

To cite this article: Chao-Yue Chen, Ting-Hai Yang, Chang-Duo Pan & Xin Wang (2019) Improved synthesis, X-ray structure, and antifungal activity of a sugar-psoralen conjugate: 4,4′-Dimethylxanthotoxol 2,3,4,6-tetra-*O*-Acetyl-β-*D*-glucoside, Journal of Carbohydrate Chemistry, 38:3, 179-191, DOI: 10.1080/07328303.2019.1609018

To link to this article: https://doi.org/10.1080/07328303.2019.1609018

Published online: 06 May 2019.

JOURNAL OF CARBOHYDRATE CHEMISTRY
2019, VOL. 38, NO. 3, 179–191
https://doi.org/10.1080/07328303.2019.1609018

Taylor & Francis
Taylor & Francis Group

Improved synthesis, X-ray structure, and antifungal activity of a sugar-psoralen conjugate: 4,4′-Dimethylxanthotoxol 2,3,4,6-tetra-*O*-Acetyl-*β*-*D*-glucoside

Chao-Yue Chen, Ting-Hai Yang, Chang-Duo Pan, and Xin Wang

School of Chemistry and Environmental Engineering, Jiangsu University of Technology, Changzhou, PR China

ABSTRACT

An improved synthesis for 4,4′-dimethylxanthotoxol 2,3,4,6-tetra-*O*-acetyl-*β*-*D*-glucoside (**1**) starting from resorcinol was developed. Crystallographic analysis of glucoside **1** indicated that the dihedral angles between the mean planes of the tricyclic ring system of adjacent molecules was 54.820(22)° probably due to the steric hindrance caused by the bulky *O*-glucoside moiety, which prevents the molecules from packing *via* $\pi\cdots\pi$ stacking between the tricyclic cores. The antifungal screening data revealed that glucoside **1** had higher inhibition than its parent compound 4,4′-dimethylxanthotoxol and azoxystrobin against *Rhizoctonia solani*, *Pyricularia grisea*, and *Alternaria alternate Japanese pear pathotype*, with the inhibitory rates of 75.4, 65.7 and 70.1%, respectively, at the 50 μg/mL concentration.

GRAPHICAL ABSTRACT

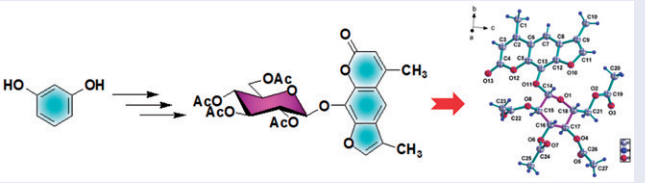

ARTICLE HISTORY
Received 7 October 2018
Accepted 10 April 2019

KEYWORDS
Antifungal activity; crystallographic analysis; glucoside; psoralen; synthesis

Introduction

Psoralens, also known as linear furocoumarins, are a group of compounds that are widely distributed in many plants. They possess a wide spectrum of biological activities, including cytotoxic, phytotoxic, photosensitizing, insecticidal, to antibacterial effects.[1–3] Furthermore, some of them have been applied as therapeutics against diseases such as skin disorders,

CONTACT Chao-Yue Chen njuchaoyuechen@163.com School of Chemistry and Environmental Engineering, Jiangsu University of Technology, Changzhou, PR China

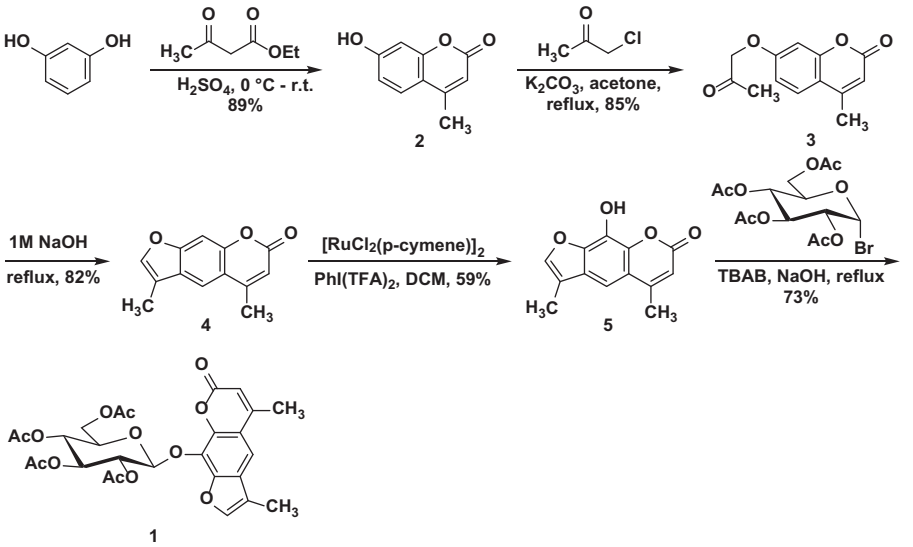

Scheme 1. Improved synthetic approach for glucoside **1**.

autoimmune diseases, cutaneous T-cell lymphoma, and several other types of cancer.[1–3] Recently, another biological effect of psoralens, *i.e.*, antifungal activity, has attracted increasing interest from agricultural chemists, because a series of structure-activity relationship (SAR) studies demonstrated that linear furanocoumarin cores could also be promising lead structures for exploiting new pesticides for the treatment of agricultural diseases.[4–10]

We have synthesized a range of glycosylated psoralen derivatives and investigated their antiproliferative effects and antioxidant activities.[3] Among those compounds, 4,4′-dimethylxanthotoxol 2,3,4,6-tetra-*O*-acetyl-*β*-*D*-glucoside (**1**, see Scheme 1) showed antiproliferative effects against three kinds of human tumor cell lines under UV light. The present paper is a continuation of our research on biologically active sugar-psoralen conjugate derivatives. Specifically, we developed an improved synthetic method for glucoside **1** and performed X-ray crystallographic analysis of glucoside **1** to obtain deeper insight into its structure. Furthermore, considering that both the furanocoumarin core[4–10] and the glycosyl moiety[11–14] have been reported as effective pharmacophores for fungicidal inhibition, the antifungal activity of glucoside **1** was further investigated to explore its potential as antifungal agent.

Results and discussion

Our previously described synthesis of glucoside **1** starting from pyrogallol took four steps to reach the key intermediate 4,4′-dimethylxanthotoxol (**5** in Scheme 1) in a 31% overall yield.[3] That method required laborious

protection/deprotection steps to restore the hydroxyl groups and suffered from unwanted side-reaction of intramolecular aldol condensation. In this work, we planned to develop a facile and more efficient procedure.

Recently, direct oxidative hydroxylation of C-H bonds by transition metals has emerged as a straight-forward and powerful strategy for generating phenols.[15–19] Prompted by this development, we envisioned a new synthetic approach for **5** starting from resorcinol and taking advantage of ruthenium(II)-catalyzed *ortho* C-H hydroxylation in order to avoid the above mentioned problems.

The modified synthetic pathway is described in Scheme 1. The preparation of key intermediate **5** began from a reaction of resorcinol with ethylacetoacetate in concentrated sulfuric acid to give 4-methyl-7-hydroxycoumarin **2** in and excellent yield (89%). This coumarin derivative was then alkylated with 1-chloroacetone in the presence of K_2CO_3 to afford 4-methyl-7-(2-oxopropoxy)-2*H*-chromen-2-one **3** in an 85% yield. Compound **3** was converted into 4,4'-dimethylpsoralen **4** after heating with 1 M NaOH in aqueous solution. In order to introduce a hydroxyl group at the 8-position of **4** regioselectively, an *ortho* C-H hydroxylation reaction was examined using transition metal catalysts such as $Pd(OAc)_2$, $Cu(OAc)_2$ and $[RuCl_2(p\text{-cymene})]_2$ under various conditions. After reaction optimization, $[RuCl_2(p\text{-cymene})]_2$ was identified as the best catalyst for *ortho*-selective hydroxylation of **4** to be converted into 4,4′-dimethylxanthotoxol **5** with $PhI(TFA)_2$ as the oxidant (59%).[17] Substituents on 7- and 9-positions may bind to the Ru catalyst and act as directing groups to enhance both the reactivity and the selectivity for adjacent C-H bond activation. As a result, the intermediate **5** was obtained in an overall 37% yield, as opposed to the originally reported overall yield of 31%.[3] Although only a 6% overall yield increase was achieved, it should be noted that the new and old routes employed different starting materials and synthetic methodologies. The previous route started from pyrogallol and a protection-deprotection strategy was necessary to reach **5**,[3] while in the new synthesis, cheaper resorcinol as starting material was employed and the key reaction was a direct oxidative hydroxylation, which avoided both the deprotection step and side-reaction of intramolecular aldol condensation in the original route. Furthermore, this new synthetic approach has the potential to be used for the synthesis of other xanthotoxols from resorcinol *via* C-H hydroxylation. The target glucoside **1** was finally obtained in a 73% yield via direct *O*-glycosylation of **5** with per-acetylglycosyl bromide in a biphasic media using tetrabutylammonium bromide (TBAB) as a phase transfer catalyst and NaOH as the base.

In order to obtain a better understanding of the structures of glycosylated psoralen derivatives, we further performed X-ray crystallographic

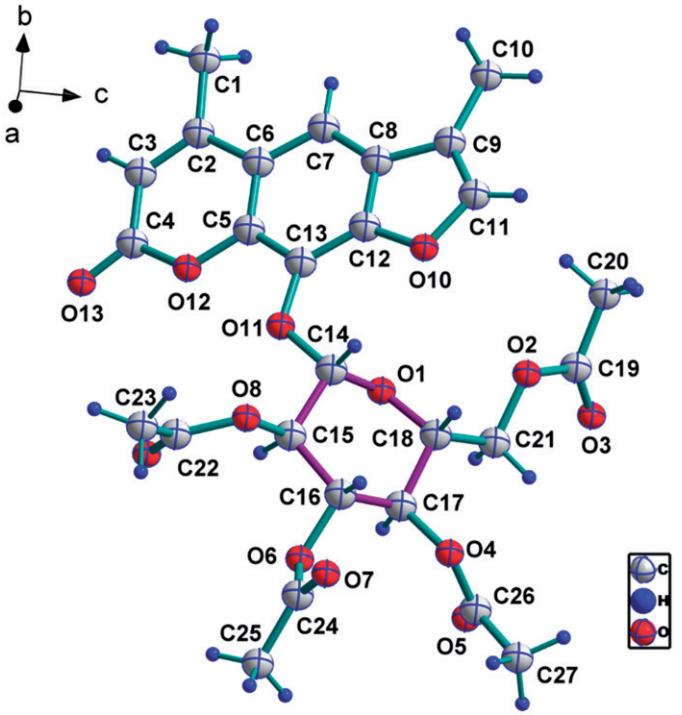

Figure 1. Molecule structure and ORTEP drawing of glucoside **1**.

analysis of glucoside **1**. The molecular structure of glucoside **1** is depicted in Figure 1. The crystallographic data are summarized in Table 1, while the selected bond lengths, bond angles, and torsion angles are given in Tables 2–4, respectively. The hydrogen bonding geometries for **1** are shown in Table 5.

As depicted in Figure 1, glucoside **1** consists of four rings in which three of them (furan, benzene, and pyrone) are fused together into a tricyclic nucleus, with a terminal glucoside ring attached to it. The dihedral angles between the furan (C8–C9–C11–O10–C12) and phenyl (C5–C6–C7–C8–C12–C13) rings, phenyl and pyrone (C2–C3–C4–O12–C5–C6) rings are 1.899(76)° and 4.032(69)°, respectively, indicating the close-to-planar structure of the tricyclic nucleus of the psoralen moiety. The two carbon atoms of the two methyl groups, C(1) and C(10), are deviated from the furan ring by 0.1172°, and from the pyrone ring by 0.0233°, respectively. It is clear that, except for the glucoside moiety, all other atoms in glucoside **1** are almost located in one big plane of π-conjugated system.

The six-membered glucoside ring (C14–C15–C16–C17–C18–O1) which attached at C13 of the aglycone is oriented approximately 45° to the plane of the psoralen ring with dihedral angle of 42.952(77)°. The Glc moiety adopts the relaxed $4C_1$ chair conformation as expected, with ring-puckering parameters of $Q = 0.587(2)$ Å, $\theta = 11.3(2)°$, and $\psi = 338.3(12)°$. All of the

Table 1. Crystal data and structure refinement for glucoside **1**.

Compound	**1**
Empirical formula	$C_{27}H_{28}O_{13}$
Chemical formula weight (Mr)	560.49
Crystal system	Orthorhombic
Space group	$P2_12_12_1$
Unit cell dimensions	
a (Å)	8.4807(4)
b (Å)	15.9662(8)
c (Å)	19.8840(9)
α (°)	90
β (°)	90
γ (°)	90
Volume (Å^3)	2692.4(2)
Z	4
Density (calcd.) g/cm^3)	1.383
Absorption coefficient (mm^{-1})	0.111
F(000)	1176
Temperature (K)	296
Radiation (Å)	Mo K_α 0.71073
θ Min, max (°)	2.4, 27.6
Data set	limiting indices $-11 < h < 11$; $-19 < k < 20$; $-20 < l < 25$
Total., Uniq. Data	24354, 6195
R (int)	0.039
N_{ref}, N_{par}	6195, 367
R, wR_2, *S*	0.0405, 0.0940, 1.05
CCDC number	1854605

Table 2. Selected bond lengths for glucoside **1**.

Bond Lengths	(Å)	Bond Lengths	(Å)
O1–C14	1.407(3)	C5-C13	1.395(3)
O1–C18	1.430(3)	C6-C7	1.398(4)
O10–C11	1.390(3)	C7-C8	1.385(3)
O10–C12	1.365(3)	C8-C9	1.443(3)
O11–C13	1.376(3)	C8-C12	1.403(3)
O11–C14	1.407(3)	C9-C10	1.499(4)
O12–C4	1.384(3)	C9-C11	1.336(4)
O12–C5	1.376(3)	C12-C13	1.387(3)
O13–C4	1.210(3)	C14-C15	1.521(3)
C2–C3	1.338(4)	C15-C16	1.521(3)
C2–C6	1.460(4)	C16-C17	1.514(3)
C3–C4	1.443(4)	C17-C18	1.527(3)
C5–C6	1.404(3)	C14-H14	0.9800

non-H substituents on the glucoside ring are situated in equatorial positions. H-14 and H-15 in the pyranose ring bear a trans-diaxial relationship to each other with torsion angle of 168.927(207)°. The glycosidic torsion angle (χ) defined by O1–C1–O11–C13 is −61.175(246)°. Based on the above analysis, it is easily observed that the glucoside moiety has the β-configuration and is the pyranose isomer. The X-ray structure determination on **1** confirms the structure proposed on the basis of the method of preparation and the ^{1}H NMR data.

A series of X-ray crystal structure analysis[20–24] of psoralens indicated that $\pi\cdots\pi$ interactions between rings of the planar tricyclic systems are a common feature in the crystal packing, thus the adjacent molecules are

Table 3. Selected bond angles for glucoside **1**.

Bond Angles	(°)	Bond Angles	(°)
C14–O1–C18	111.33(16)	O10–C11–C9	112.8(2)
C11–O10–C12	105.28(18)	O10–C12–C8	110.3(2)
C13–O11–C14	120.55(17)	O10–C12–C13	127.5(2)
C4–O12–C5	121.3(2)	C8–C12–C13	122.2(2)
C3–C2–C6	118.9(2)	O11–C13–C5	115.4(2)
C2–C3–C4	123.1(2)	O11–C13–C12	128.7(2)
O12–C4–O13	116.2(3)	C5–C13–C12	115.9(2)
O12–C4–C3	117.1(2)	O1–C14–O11	108.11(18)
O13–C4–C3	126.7(2)	O1–C14–C15	108.82(18)
O12–C5–C6	121.7(2)	O11–C14–C15	105.18(17)
O12–C5–C13	115.0(2)	C14–C15–C16	111.23(18)
C6–C5–C13	123.2(2)	C15–C16–C17	112.03(19)
C2–C6–C5	117.6(2)	C16–C17–C18	109.89(18)
C2–C6–C7	123.1(2)	O1–C18–C17	106.64(17)
C5–C6–C7	119.3(2)	C8–C9–C11	105.8(2)
C6–C7–C8	118.4(2)	O1–C14–H14	111.00
C7–C8–C9	133.3(2)	O11–C14–H14	112.00
C7–C8–C12	121.0(2)	C15–C14–H14	111.00
C9–C8–C12	105.7(2)		

Table 4. Selected torsion angles for glucoside **1**.

Torsion Angles	(°)	Torsion Angles	(°)
C18–O1–C14–O11	178.94(16)	C11–O10-C12-C8	−0.7(3)
C12–O10–C11–C9	0.2(3)	C11–O10-C12-C13	178.1(2)
C13–O11–C14–C15	−177.3(2)	C13–O11-C14-O1	−61.2(3)
C14–O11–C13–C12	−12.5(4)	C14–O11-C13-C5	168.6(2)
C5–O12–C4–C3	−4.2(3)	C4–O12-C5-C13	−177.9(2)
C5–O12–C4–O13	176.3(2)	C4–O12-C5-C6	2.4(3)
C3–C2–C6–C7	173.3(2)	C6–C2-C3-C4	3.5(4)
C2–C3–C4–O13	−179.4(3)	C3–C2-C6-C5	−5.3(4)
O12–C5–C6–C7	−176.2(2)	C2–C3-C4-O12	1.2(4)
C13–C5–C6–C7	4.1(4)	O12–C5-C6-C2	2.4(4)
O12–C5–C13–O11	−4.4(3)	C6–C5-C13-C12	−3.8(4)
O12–C5–C13–C12	176.5(2)	C6–C5-C13-O11	175.3(2)
C2–C6–C7–C8	−179.3(2)	C13–C5-C6-C2	−177.3(2)
C6–C7–C8–C12	−2.6(4)	C5–C6-C7-C8	−0.8(4)
C9–C8–C12–C13	−178.0(2)	C6–C7-C8-C9	178.6(3)
C12–C8–C9–C11	−0.7(3)	C7–C8-C9-C11	178.3(3)
C8–C9–C11–O10	0.3(3)	C9–C8-C12-O10	0.9(3)
C8–C12–C13–C5	0.2(4)	C7–C8-C12-C13	2.9(4)
C8–C12–C13–O11	−178.7(2)	C7–C8-C12-O10	−178.3(2)
O1–C14–C15–C16	53.6(3)	O10–C12-C13-O11	2.7(4)
O11–C14–C15–C16	169.22(19)	O10–C12-C13-C5	−178.4(2)
C15–C16–C17–C18	49.7(3)	C14–C15–C16–C17	−46.6(3)
C18–O1–C14–C15	−67.3(2)	C16–C17–C18–O1	−59.2(2)
C14–O1–C18–C17	70.1(2)		

usually packed in near parallel arrangements across centers the of tricyclic moieties. However, the crystallographic data of glucoside **1** indicate that the molecules are stabilized only by weak C–H···O interactions (Table 5), and no $\pi\cdots\pi$ stacking between rings of the tricyclic systems in adjacent molecules is observed in it (Figure 2). In fact, the dihedral angles between the mean planes of the tricyclic ring system of adjacent molecules is 54.820(22)°. It is obvious that the steric hindrance caused by the bulky

Table 5. Geometry for hydrogen bonds in the crystal structure of glucoside **1**.

D—H···A	D—H	H···A	D···A	D—H···A
C1—H1B···O4	0.9600	2.5300	3.250(3)	132.00
C14— H14···O10	0.9800	2.5400	2.912(3)	102.00
C15—H15···O9	0.9800	2.2800	2.721(3)	106.00
C16—H16···O7	0.9800	2.2700	2.706(3)	106.00
C17—H17···O5	0.9800	2.3300	2.714(3)	102.00
C20—H20B···O13	0.9600	2.4200	3.286(4)	150.00
C23—H23C···O3	0.9600	2.3200	3.134(4)	142.00
C25—H25C···O5	0.9600	2.5400	3.484(4)	169.00

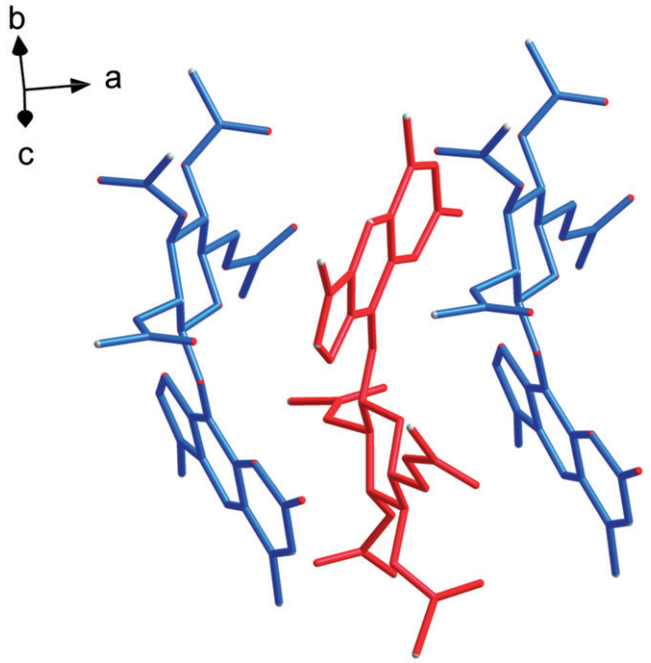

Figure 2. Molecular packing of glucoside **1**.

O-glucoside moiety may be responsible for the disruption of $\pi\cdots\pi$ stacking interactions between the tricyclic ring aglycones in glucoside **1**.

We also evaluated the *in vitro* antifungal activities of glucoside **1** and compared it to the parent compound **5** by mycelium growth rate method[5] against the six most common plant pathogenic fungi in China, including *Rhizoctonia solani*, *Pyricularia grisea*, *Gibberella zeae*, *Alternaria solani*, *Alternaria alternate*, and *Fusarium oxysporum f. sp. Niveum*. The positive control used was azoxystrobin, and the results are presented in Table 6. Both **1** and **5** were more active than the positive control against *Rhizoctonia solani*, *Pyricularia grisea*, and *Alternaria alternata Japanese pear pathotype*, and both displayed equivalent antifungal activity as the positive control against *Fusarium oxysporum f. sp. niveum* but showed poorer activity than the positive control against *Gibberella zeae* and *Alternaria solani*. In addition, glucoside **1** revealed higher inhibition than

Table 6. Antifungal activities of compounds **1** and **5** against six fungus species *in vitro*[a].

	Species[b]/ Inhibitory Rate (%)[c]					
Compound number	RHS	PYG	GIZ	ALS	AAJPP	FON
1	75.4	65.7	18.7	12.6	70.1	31.7
5	67.3	59.2	20.2	10.3	66.5	30.4
Azoxystrobin	61.2	52.8	59.3	30.4	62.0	32.2

[a]RHS: *Rhizoctonia solani*; PYG: *Pyricularia grisea*; GIZ: *Gibberella zeae*; ALS: *Alternaria solani*; AAJPP: *Alternaria alternata Japanese pear pathotype*; FON: *Fusarium oxysporum f. sp. Niveum*.
[b]Compound concentration: 50 μg/mL.
[c]All data were presented as the average of three replications.

its parent compound **5** against *Rhizoctonia solani*, *Pyricularia grisea*, and *Alternaria alternata Japanese pear pathotype* under the same conditions, suggesting that the introduction of a glycoside moiety[11–14] is helpful to improve the antifungal activity of furancoumarins for these fungi. These preliminary results indicate the potential of using glycosylated psoralen derivatives for new furancoumarin fungicide design, and further investigations are currently underway in our lab.

Conclusion

4,4′-Dimethylxanthotoxol 2,3,4,6-tetra-*O*-acetyl-*β*-*D*-glucoside **1** was synthesized *via* a C-H hydroxylation methodology starting from resorcinol. Crystal structure analysis of **1** revealed that probably owning to the steric effect of the bulky terminal *O*-glucoside moiety, this molecule does not have $\pi\cdots\pi$ stacking interactions between the tricyclic nucleus of the aglycone in adjacent molecules. We have also shown that among the six kinds of phytopathogenic fungi tested, glucoside **1** was particularly effective against *Rhizoctonia solani*, *Pyricularia grisea*, and *Alternaria alternata Japanese pear pathotype* with the inhibitory rates of 75.4, 65.7 and 70.1%, *vs* 61.2, 52.8 and 62.0% for the positive control of azoxystrobin, respectively, at the concentration of 50 μg/mL.

Experimental section

General methods

Chemicals were purchased as reagent grade and used without further purification. Thin-layer chromatography (TLC) was carried out on glass plates coated with silica gel (Qingdao Haiyang Chemical Co., Gel 60 F-254) and visualized by UV light (254 nm and 365 nm). Melting points were determined on an electrically heated RK-Z melting point apparatus (Analytical instrument factory in Tianjin, China) and were uncorrected. ^{1}H and ^{13}C NMR spectra were determined on Brucker ARX-300 (300 MHz, Bruker, Rheinstetten/Karlsruhe, Germany) with TMS as internal standard.

Synthesis of 7-hydroxy-4-methylcoumarin (2)

To a concentrated H_2SO_4 (80.0 mL) at 0 °C, a solution of resorcinol (7.71 g, 70.0 mmol) in freshly distilled ethyl acetoacetate (9.11 g, 70.0 mmol) was added dropwise. The reaction mixture was allowed to warm to room temperature and stirred over night. Then, the mixture was poured with vigorous stirring into ice water (100.0 mL). The solid was collected by filtration, washed with ice-cold water, and recrystallized from ethanol to afford pure 7-hydroxy-4-methylcoumarin **2** as a white solid. Yield 89%, m.p. 182–184 °C (Lit. 188 °C[25]). ^{1}H NMR (300 MHz, DMSO-d_6) δ(ppm): 10.50 (s, 1 H), 7.58 (d, J = 6.0 Hz, 1 H), 6.79 (d, J = 6.0 Hz, 1 H), 6.69 (s, 1 H), 6.11 (s, 1 H), 2.35 (s, 3 H).

Synthesis of 7-(2-oxo-propoxy)-4-methyl-2H-chromen-2-one (3)

To the mixture of 7-hydroxy-4-methylcoumarin **2** (5.46 g, 31.0 mmol), anhydrous K_2CO_3 (8.55 g, 62.0 mmol), and catalytic amount of KI in dry acetone (50.0 mL), chloroacetone (4.16 g, 45.0 mmol) was added dropwise with vigorous stirring at room temperature. After the addition was complete, the reaction mixture was refluxed for 24 h (monitored by TLC). Then, the mixture was cooled and filtered. The filtrate was evaporated under reduced pressure and the residue was crystallized from MeOH to give 7-(2-oxo-propoxy)-4-methyl-2*H*-chromen-2-one **3** as a white solid. Yield 85%, m.p. 160 – 163 °C (Lit. 155–158 °C[26]). ^{1}H NMR (300 MHz, $CDCl_3$) δ (ppm): 7.53 (d, J = 9.0 Hz, 1 H), 6.88 (dd, J = 9.0, 3.0 Hz, 1 H), 6.74 (d, J = 3.0 Hz, 1 H), 6.15 (s, 1 H), 4.64 (s, 2 H), 2.39 (s, 3 H), 2.30 (s, 3 H).

Synthesis of 4,4′-dimethylpsoralen (4)

7-(2-Oxo-propoxy)-4-methyl-2*H*-chromen-2-one **3** (5.81 g, 25.0 mmol) was dissolved in aqueous NaOH (1.0 M, 100.0 mL) and refluxed for 24 h under nitrogen atmosphere. The mixture was cooled to 0 °C and then acidified with 2.0 M HCl. The precipitation formed was collected, washed with cold water. The crude product was purified by silica gel chromatography with petroleum ether/ethyl acetate (1:1) to give 4,4'-dimethylpsoralen **4** as a white solid. Yield 82%, m.p. 219–221 °C (Lit. 220–222 °C[27]). ^{1}H NMR (300 MHz, $CDCl_3$) δ (ppm): 7.67 (s, 1 H), 7.46 (s, 1 H), 7.39 (s, 1 H), 6.25 (s, 1 H), 2.52 (s, 3 H), 2.29 (s, 3 H). ^{13}C NMR (75 MHz, $CDCl_3$) δ (ppm): 161.3, 156.7, 152.9, 151.7, 143.2, 126.5, 116.2, 115.7, 114.8, 113.3, 99.8, 19.3, 8.0.

Synthesis of 4,4′-dimethylxanthotoxol (5)

4,4'-Dimethylpsoralen **4** (0.107 g, 0.50 mmol), $[RuCl_2(p\text{-cymene})]_2$(7.7 mg, 2.5 mol %), $PhI(TFA)_2$ (0.43 g, 1.0 mmol) and DCE (15.0 mL) were placed into a 50.0 mL schlenk tube equipped with a septum under N_2. The tube was then placed into an oil bath and the reaction mixture was stirred at reflux for 24 h. At ambient temperature, the reaction mixture was diluted with H_2O (15.0 mL) and extracted with EtOAc (3 x 15.0 mL). The combined organic layer was concentrated under reduced pressure. The crude products were purified by column chromatography (*n*-hexane/EtOAc) on silica gel to afford the desired product. Yield 59%, m.p. > 250 °C (Lit. >300 °C[28]). ^{1}H NMR (300 MHz, DMSO-d_6) δ(ppm): 10.49 (s, 1 H), 7.82 (s, 1 H), 7.40 (s, 1 H), 6.30 (s, 1 H), 2.48 (s, 3 H), 2.22 (s, 3 H). ^{13}C NMR (75 MHz, DMSO-d_6) δ(ppm): 160.4, 154.7, 145.8, 143.9, 140.1, 130.4, 126.9, 117.2, 116.3, 112.8, 105.8,19.3, 8.0.

Synthesis of 4,4′-Dimethyl-8-O-(2′′,3′′,4′′,6′′-tetra-O-acetyl-β-D-glucopyranosyl)xanthotoxol (1)

4,4′-Dimethylxanthotoxol **5** (1.38 g, 6.0 mmol), tetra-acetylglucosyl bromide (3.08 g, 7.5 mmol), and TBAB (2.58 g, 8.0 mmol) were dissolved in DCM (30.0 mL) and warmed to 35 °C. A solution of NaOH (5%, 10.0 mL) was added, and the reaction mixture was refluxed for 8 h. The mixture was cooled to room temperature and diluted with $CHCl_3$ (30.0 mL), which was then washed with cold 1.0 N HCl solution and brine, dried over anhydrous Na_2SO_4, and concentrated. The residue was purified by column chromatography (silica gel, EtOAc:hexane = 1:2 as eluent) to afford glycosylated psoralen derivative **1**. Yield 73%, white solid, m.p. 118 – 120 °C (Lit. 118-120 °C [3]). ^{1}H NMR (300 MHz, $CDCl_3$) δ(ppm): 7.48(d, J = 1.2 Hz, 1 H), 7.47 (s, 1 H), 6.25 (d, J = 1.2 Hz, 1 H), 5.45 – 5.21 (m, 4 H), 4.26 (dd, J = 12.0, 4.5 Hz, 1 H), 4.08 (dd, J = 12.0, 3.9 Hz, 1 H), 3.75 (ddd, J = 9.9, 4.8, 2.1 Hz, 1 H), 2.51 (d, J = 0.9 Hz, 3 H), 2.27 (d, J = 1.2 Hz, 3 H), 2.19 (s, 3 H), 2.05 (s, 3 H), 2.02 (s, 3 H), 1.97 (s, 3 H). ^{13}C NMR (75 MHz, $CDCl_3$) δ(ppm): 170.6, 170.2, 169.8, 169.4, 159.9, 152.7, 148.6, 143.4, 128.5, 127.2, 117.2, 115.9, 113.5, 110.3, 101.6, 72.7, 72.1, 71.4, 68.4, 61.7, 30.9, 20.7, 20.62, 20.58, 19.4, 7.7.

X-ray crystallography

X-Ray crystallography measurements were made on a Bruker Apperx II diffractometer with graphite-monochromated Mo-K_α radiation (λ = 0.71073 Å). An analytical crystalline sample of glucoside (**1**) was obtained by recrystallization from *n*-hexane/ethyl acetate mixture.

The structure was solved by direct methods, and the non-hydrogen atoms were located from the trial structure and then refined anisotropically with SHELXTL using full-matrix least-squares procedures based on F^2 values. Hydrogen atoms positions were fixed geometrically at calculated distances and allowed to ride on the parent atoms. CCDC reference number 1854605 contains the supplementary crystallographic data reported in this paper as CIF files. These data sets can be obtained free of charge from The Cambridge Crystallographic Data Center via www.ccdc.cam.ac.uk/data_request/cif, and are also available as supporting information.

Antifungal assay

The antifungal activities of the glucoside **1** and its parent compound **5** were evaluated *in vitro* against six plants pathogenic fungi (*Rhizoctonia solani*, *Pyricularia grisea*, *Gibberella zeae*, *Alternaria solani*, *Alternaria alternata Japanese pear pathotype*, *Fusarium oxysporum f. sp. niveum*), using the mycelium growth inhibitory rate method[5] on PDA (a kind of culture medium which was prepared with 200 g of potato, 20 g of agar, and 20 g of Dextrose per liter of distilled water). The commercially available azoxystrobin, a broad spectrum fungicide used for protecting plants and food crops from fungal diseases, was used as positive control. The tested compounds were dissolved in dimethyl formamide (DMF) to generate the stock solution before mixing with molten agar below 55 °C. The medium containing compounds at a concentration of 50 μg/mL for the preliminary screening was poured into sterilized petri dishes. Mycelia disks (5 mm in diameter) were then inoculated in the center of the Petri dishes and incubated at 25 °C for 3 to 5 days. A negative control was maintained with sterile water mixed with PDA medium. Each treatment had three replicates. The diameter of colony growth was measured when the fungal growth in the control had completely covered the Petri dishes. The inhibition percentage of mycelia growth was calculated using the following formula:

$$\text{Mycelia growth inhibition } (\%) = \frac{D_a - D_b}{D_a} \times 100$$

Where D_a represents control colony diameter and D_b represents treated colony diameter. The colony diameter is in millimeters. The colony diameter of each strain was measured by cross bracketing method.

Funding

This work was supported in parts by the Natural Science Foundation of China (grant number 21602086) and the Changzhou Sci&Tech Program (grant number CJ20179015).

References

[1] Melough, M. M.; Cho, E.; Chun, O. K. Furocoumarins: a review of biochemical activities, dietary sources and intake, and potential health risks. *Food Chem. Toxicol.* **2018**, *113*, 99–107. doi:10.1016/j.fct.2018.01.030.

[2] Francisco, C. S.; Rodrigues, L. R.; Cerqueira, N. M. F. S. A.; Oliveira-Campos, A. M. F.; Rodrigues, L. M.; Esteves, A. P. Synthesis of novel psoralen analogues and their in vitro antitumor activity. *Bioorg. Med. Chem.* **2013**, *21*, 5047–5053. doi:10.1016/j.bmc.2013.06.049.

[3] Chen, C. Y.; Sun, J. G.; Liu, F. Y.; Fung, K. P.; Wu, P.; Huang, Z. Z. Synthesis and biological evaluation of glycosylated psoralen derivatives. *Tetrahedron* **2012**, *68*, 2598–2606. doi:10.1016/j.tet.2012.01.090.

[4] Sardari, S.; Nishibe, S.; Daneshtalab, M. Coumarins, the bioactive structures with antifungal property. *Stud. Nat. Prod. Chem.* **2000**, *23*, 335–393.

[5] Yu, X.; Wen, Y.; Liang, C. G.; Liu, J.; Ding, Y. B.; Zhang, W. H. Design, synthesis and antifungal activity of psoralen derivatives. *Molecules* **2017**, *22*, 1672. doi:10.3390/molecules22101672.

[6] Zhang, M. Z.; Zhang, R. R.; Wang, J. Q.; Eur, J. Microwave-assisted synthesis and antifungal activity of novel fused Osthole derivatives. *Eur. J. Med. Chem.* **2016**, *97*, 275–279. doi:10.21037/atm.2016.05.14.

[7] Xiao, L.; Zhou, Y. M.; Zhang, X. F.; Du, F. Y. Notopterygium incisum extract and associated secondary metabolites inhibit apple fruit fungal pathogens. *Pestic. Biochem. Physiol.* **2018**, *150*, 59–65.

[8] Song, P. P.; Zhao, J.; Liu, Z. L.; Duan, Y. B.; Hou, Y. P.; Zhao, C. Q.; Wu, M.; Wei, M.; Wang, N. H.; Lv, Y.; Zhao, J. H. Evaluation of antifungal activities and structure-activity relationships of coumarin derivatives. *Pest Manag. Sci.* **2017**, *73*, 94–101. doi:10.1002/ps.4422.

[9] Xie, Q.; Li, S. X.; Liao, D. F.; Wang, W.; Tekwani, B.; Huang, H. Y.; Ali, A.; Rehman, J.; Schrader, K. K.; Duke, S. O.; et al. Bio-pesticidal and Antimicrobial Coumarins from Angelica dahurica (Fisch. Ex Hoffm). *Rec. Nat. Prod* **2016**, *10*, 294–306.

[10] Nam, V. D.; Teruhisa, F.; Hirofumi, T.; Hiroshi, K.; Khoi, N. M.; Dung, L. V.; Ha, D. T.; Hiroshi, H. Chemical composition of clausena lansium (lour.) skeels leaves and antifungal activity. *Nat. Prod. Sci.* **2016**, *22*, 35–40. doi:10.20307/nps.2016.22.1.35.

[11] Hipólito, T. M. M.; Bastos, G. T. L.; Barbosa, T. W. L.; de Souza, T. B.; Coelho, L. F. L.; Dias, A. L. T.; Rodríguez, I. C.; dos Santos, M. H.; Dias, D. F.; Franco, L. L.; Carvalho, D. T. Synthesis, activity, and docking studies of eugenol-based glucosides as new agents against Candida sp. *Chem. Biol. Drug Des.* **2018**, *92*, 1514–1524. doi:10.1111/cbdd.13318.

[12] de Souza, T. B.; Orlandi, M.; Coelho, L. F. L.; Malaquias, L. C. C.; Dias, A. L. T.; Carvalho, R. R.; Silva, N. C.; Carvalho, D. T. Synthesis and in vitro evaluation of antifungal and cytotoxic activities of eugenol glycosides. *Med. Chem. Res.* **2014**, *23*, 496–502. doi:10.1007/s00044-013-0669-2.

[13] de Souza, T. B.; Raimundo, P. O. B.; Andrade, S. F.; Hipólito, T. M. M.; Silva, N. C.; Dias, A. L. T.; Ikegaki, M.; Rocha, R. P.; Coelho, L. F. L.; Veloso, M. P.; et al. Synthesis and antimicrobial activity of 6-triazolo-6-deoxy eugenol glucosides. *Carbohydr. Res.* **2015**, *410*, 1–8. doi:10.1016/j.carres.2015.04.002.

[14] Vudhgiri, S.; Koude, D.; Veeragoni, D. K.; Misra, S.; Prasad, R. B. N.; Jala, R. C. R. Synthesis and biological evaluation of 5-fatty-acylamido-1, 3, 4-thiadiazole-2-thioglycosides. *Bioorg. Med. Chem. Lett.* **2017**, *27*, 3370–3373. doi:10.1016/j.bmcl.2017.06.004.

[15] Li, X.; Liu, Y. H.; Gu, W. J.; Li, B.; Chen, F. J.; Shi, B. F. Copper-mediated hydroxylation of arenes and heteroarenes directed by a removable bidentate auxiliary. *Org. Lett.* **2014**, *16*, 3904–3907. doi:10.1021/ol5016064.

[16] Mo, F.; Trzepkowski, L. J.; Dong, G. Synthesis of ortho-acylphenols through the palladium-catalyzed ketone-directed hydroxylation of arenes. *Angew. Chem. Int. Ed. Engl.* **2012**, *51*, 13075–13079. doi:10.1002/anie.201207479.

[17] Liu, W.; Ackermann, L. Ortho- and para-selective ruthenium-catalyzed C(sp2)-H oxygenations of phenol derivatives. *Org. Lett.* **2013**, *15*, 3484–3486. doi:10.1021/ol401535k.

[18] Alonso, D. A.; Najera, C.; Pastor, I. M.; Yus, M. Transition-metal-catalyzed synthesis of hydroxylated arenes. *Chemistry* **2010**, *16*, 5274–5284. doi:10.1002/chem.201000470.

[19] Yang, F.; Zhang, H.; Liu, X.; Wang, B.; Ackermann, L. Transition metal-catalyzed regio-selective aromatic C—H bond oxidation for C—O bond formation. *Chin. J. Org. Chem.* **2019**, *39*, 59–73. doi:10.6023/cjoc201808017.

[20] Lei, L.; Xue, Y. B.; Liu, Z.; Peng, S. S.; He, Y.; Zhang, Y.; Fang, R.; Wang, J. P.; Luo, Z. W.; Yao, G. M.; et al. Coumarin derivatives from Ainsliaea fragrans and their anticoagulant activity. *Sci. Rep* **2015**, *5*, 13544.

[21] Cox, P. J.; Jaspars, M.; Kumarasamy, Y.; Nahar, L.; Sarker, S. D.; Shoeb, M. A mixed crystal of imperatorin and phellopterin, with C–H.O, C–H.pi and pi-pi Interactions. *Acta Cryst.* **2003**, *59*, o520–o522.

[22] Bauri, A. K.; Foro, S.; Nhu Do, Q. N. Crystal structure of bergapten: a photomutagenic and photobiologically active furanocoumarin. *Acta Crystallogr. E Cryst. Commun.* **2016**, *E72*, 1194–1196. doi:10.1107/S2056989016011221.

[23] Magotra, D. K.; Gupta, V. K.; Goswami, K. N.; Thappa, R. K. Archangelin. *Acta Cryst* **1995**, *C51*, 2196–2198.

[24] Brisse, F.; Simard, M. G.; Dugas, H.; Basak, A. Structure of a psoralen derivative of a monosubstituted 18-crown-6 ether. *Acta Crystallogr. C Cryst. Struct. Commun.* **1991**, *C47*, 1683–1687. doi:10.1107/S0108270190013725.

[25] Lingaraju, G. S.; Balaji, K. S.; Jayarama, S.; Anil, S. M.; Kiran, K. R.; Sadashiva, M. P. Synthesis of new coumarin tethered isoxazolines as potential anticancer agents. *Bioorg. Med. Chem. Lett.* **2018**, *28*, 3606–3612. doi:10.1016/j.bmcl.2018.10.046.

[26] Soni, J. N.; Soman, S. S. Synthesis and antimicrobial evaluation of amide derivatives of benzodifuran-2-carboxylic acid. *Eur. J. Med. Chem.* **2014**, *75*, 77–81. doi:10.1016/j.ejmech.2014.01.026.

[27] Shen, Q.; Peng, Q.; Shao, J.; Liu, X.; Huang, Z.; Pu, X.; Ma, L.; Li, Y. M.; Chan, A. S.; Gu, L. Synthesis and biological evaluation of functionalized coumarins as acetylcholinesterase inhibitors. *Eur. J. Med. Chem.* **2005**, *40*, 1307–1315. doi:10.1016/j.ejmech.2005.07.014.

[28] Marzaro, G.; Gandin, V.; Marzano, C.; Guiotto, A.; Chilin, A. Psoralenquinones as a novel class of proteasome inhibitors: design, synthesis and biological evaluation. *ChemMedChem* **2011**, *6*, 996–1000. doi:10.1002/cmdc.201100041.